Microchimica Acta (2019) 186: 320
https://doi.org/10.1007/s00604-019-3423-8

ORIGINAL PAPER

Spectrophotometric determination of the activity of alkaline phosphatase and detection of its inhibitors by exploiting the pyrophosphate-accelerated oxidase-like activity of nanoceria

Pengjuan Ni[1] · Junfeng Xie[2] · Chuanxia Chen[1] · Yuanyuan Jiang[1] · Zhenlu Zhao[1] · Yan Zhang[3] · Yizhong Lu[1] · Jinghua Yu[3]

Received: 6 December 2018 / Accepted: 8 April 2019 / Published online: 2 May 2019

Abstract

The oxidase-like activity of nanoceria is low. This limits its practical applications. It is demonstrated here that pyrophosphate ion (PPi) can improve the oxidase-like activity of nanoceria. Specifically, nanoceria catalyzes the oxidation of colorless 3,3′,5,5′-tetramethylbenzidine (TMB) to give a blue product (oxTMB) with an absorption peak at 645 nm in the presence of PPi. If, however, alkaline phosphatase (ALP) is present, it will hydrolyze PPi, and this results in a decreased oxidase-like activity of nanoceria. Hence, less blue oxTMB willl be formed. On the other hand, if the ALP inhibitor Na_3VO_4 is added to the system, the oxidase-like activity of nanoceria is gradually restored. On the basis of the above results, a spectrophotometric method was developed for determination of the activity of ALP. It works in the 0.5 to 10 $mU.mL^{-1}$ activity range and has a 0.32 $mU.mL^{-1}$ detection limit. Na_3VO_4 causes a 50% ALP inhibition if present in 71 μM concentration. The assay was successfully applied to the determination of ALP in spiked human serum and gave good recoveries.

Keywords Cerium oxide nanoparticles · Nanozymes · Oxidase mimetics · 3,3′,5,5′-Tetramethylbenzidine · Sodium vanadate · Inhibitor

Introduction

Alkaline phosphatase (ALP), an essential and universal enzyme in mammalian body fluids and tissues, can dephosphorylate phosphoryl esters into inorganic phosphates in metabolic pathways [1]. As a result, ALP plays key roles in many cellular functions through the dephosphorylation of proteins [2]. The abnormal level of ALP is closely associated with several diseases, such as bone disease [3], liver dysfunction [4], breast and prostate cancers [5] and diabetes [6]. Thus, developing highly sensitive methods for ALP activity detection is of great significance.

To date, many analytical methods have been established for ALP activity detection, including spectrophotometry [7], fluorimetry [8], electrochemistry [9], surface-enhanced Raman scattering method [10] and chemiluminescence [11]. Among them, spectrophotometry is much more attractive due to its simplicity, easy readout and low cost. The most widely used spectrophotometric method for ALP activity detection in clinical laboratories is based on the ALP-catalyzed *p*-nitrophenyl phosphate to *p*-nitrophenol with an intense absorption band at

Electronic supplementary material The online version of this article (https://doi.org/10.1007/s00604-019-3423-8) contains supplementary material, which is available to authorized users.

✉ Pengjuan Ni
mse_nipj@ujn.edu.cn

✉ Yizhong Lu
mse_luyz@ujn.edu.cn

✉ Jinghua Yu
ujn.yujh@gmail.com

[1] School of Materials Science and Engineering, University of Jinan, Jinan 250022, China

[2] College of Chemistry, Chemical Engineering and Materials Science, Key Laboratory of Molecular and Nano Probes (Ministry of Eduction), Collaborative Innovation Center of Functionalized Probes for Chemical Imaging in University of Shandong, Institute of Molecular and Nano Science, Shandong Normal University, Jinan 250014, China

[3] School of Chemistry and Chemical Engineering, University of Jinan, Jinan 250022, China

405 nm. Though this method is simple and efficient, it suffers from low selectivity and poor anti-interference ability [12]. By using ascorbic acid 2-phosphate (AAP) as the ALP substrate, another kind of spectrophotometric method for ALP activity detection is carried out. In this method, AAP is hydrolyzed to form ascorbic acid that can reduce silver ions to the metal silver and coats on the surface of Au nanorod or nanostar, resulting in a blueshift in longitudinal localized surface plasmon resonance peak of Au nanorod or nanostar with obvious color changes [13, 14]. Although these methods show high sensitivity, the preparation procedures for Au nanorod or nanostar are time-consuming and complex. In order to overcome these shortcomings, Shi et al. reported a spectrophotometric method for ALP detection without the preparation of nanomaterials based on the Cu(II)-horseradish peroxidase (HRP)-3,3′,5,5′-tertramethylbenzidine (TMB)-H_2O_2 system [15]. Despite its simplicity in operation only by mixing all these reagents together, it is limited by the utilization of HRP due to its time-consuming separation and purification. As alternatives of nature enzymes, nanozymes (nanomaterials with enzyme activity) especially the peroxidase and oxidase mimetics have attracted great attention due to their easy preparation, low cost and high stability over the past years [16, 17]. Peroxidase mimetics, such as Cu-MOFs and Cu(II)-G_{20} have been used for spectrophotometric detection of ALP [18, 19]. These nanozymes are found to be promising candidates in the construction of spectrophotometric method. The oxidase mimetics can oxidize the peroxidase substrates (such as TMB) directly without the addition of unstable H_2O_2, which makes them a much simpler choose than peroxidase mimetics-based spectrophotometric methods. However, to one's disappointment, few nanozymes show the oxidase-like activity [20–22].

The best example of oxidase mimetics is CeO_2 nanoparticles (nanoceria) that is firstly reported in 2009 [23]. Since then, nanoceria has received extensive attention. However, the nanoceria usually shows low oxidase-like activity. Therefore, great efforts have been paid to enhance its catalytic activity. For example, the oxidase-like activity of nanoceria can be improved by the aid of fluoride capping [24], protons [25], sulfate ions [26] and nucleoside triphosphates [27]. Inspired by the previous success of the modulation of nanozymes activity, here, we find an interesting fact that the oxidase-like activity of nanoceria can be significantly accelerated by the introduction of pyrophosphate (PPi). It is found that the catalytic activity of nanoceria towards TMB is dramatically enhanced after the addition of PPi to the detection system. In the presence of ALP, PPi is hydrolyzed to phosphate (Pi) that triggers the decrease of the oxidase-like activity of nanoceria. While, when the ALP is firstly incubated with its inhibitor Na_3VO_4, the hydrolysis of PPi is greatly inhibited and thus the oxidase-like activity recover. Based on these facts, a highly sensitive and selective assay for ALP and Na_3VO_4 is established.

Experimental section

Chemicals and materials

Sodium orthovanadate, potassium antimony tartrate, lysozyme, pepsin and pancreatin were purchased from Shanghai Macklin Biochemical Co., Ltd. (Shanghai, China, www.macklin.cn). Sodium pyrophosphate, sodium citrate, ethylenediaminetetraacetic acid (EDTA), ammonium molybdate tetrahydrate, bovine serum albumin (BSA), trypsin, TMB and magnesium chloride were obtained from Aladdin Reagent Company (Shanghai, China, www.aladdin-e.com). ALP, ascorbic acid (AA) and Trizma base were acquired form Sigma-Aldrich (St. Louis, USA, www.sigmaaldrich.com). Cerium nitrate and ammonium hydroxide (50% *v*/v aqueous solution) were obtained from Alfa Aesar (Tianjin, China, www.alfa.com). All these reagents were used as received. Ultrapure water was used throughout all the experiments. The preparation procedure of nanoceria method and its characterization (Fig. S1) of nanoceria were shown in the electronic supporting material.

Apparatus

UV-vis absorption spectra were collected using a UV-8000 spectrophotometer (Shanghia Metash Instruments Co.,Ltd., China, www.metash.com). Transmission electron microscopy (TEM) images were obtained on JEM-2010, 200 kV (JEOL Ltd., Japan, www.jeol.co.jp). Powder X-ray diffraction (XRD) patterns was conducted on a Bruker diffractometer with Cu Kα radiation (D8 Advanced X-ray diffractometer, λ = 1.5406 Å) (Bruker Corporation, Germany, www.bruker.com).

Determination of ALP activity and inhibition by Na_3VO_4

For the spectrophotometric detection of ALP, 70 μL of Tris-HCl buffer (pH 7.4), 10 μL of 7 mM PPi, 10 μL of 1 mM $MgCl_2$ and 10 μL of various concentrations of ALP were added sequentially into a 1.5 mL calibrated test tube and incubated at 37 °C for 1 h. Then, 700 μL of acetate buffer (pH 4.0), 100 μL of 2.5 mg mL^{-1} nanoceria and 100 μL of 5 mM TMB were added individually. The solutions were allowed to stand at 37 °C for 3 min the UV-vis absorption spectra measurement by scanning from 550 to 750 nm and the maximum absorbance at 645 nm is used for quantitative analysis.

For Na_3VO_4 detection, 60 μL of Tris-HCl buffer (pH 7.4), 10 μL of 2 U mL^{-1} ALP and 10 μL of different concentrations of Na_3VO_4 were added sequentially into a 1.5 mL calibrated test tube and incubated at 37 °C for 30 min. Then, 10 μL of 7 mM PPi were introduced and incubated for another 1 h. After that, 700 μL of acetate buffer (pH 4.0), 100 μL of

2.5 mg mL^{-1} nanoceria and 100 μL of 5 mM TMB were added, mixed thoroughly and incubated at 37 °C for 3 min. Finally, the mixture was transferred for the UV-vis absorption spectra measurements.

The phosphatase-like activity of nanoceria

To investigate the phosphatase-like activity of nanoceria, 80 μL of Tris-HCl buffer (pH 7.4), 10 μL of 7 mM PPi, 110 μL of distilled water and 100 μL of 2.5 mg mL^{-1} nanoceria were added sequentially into a 1.5 mL calibrated test tube containing 700 μL of acetate buffer (pH 4.0) and incubated at 37 °C for 3 min. Then, 100 μL of the above mixture was added into a 1.5 mL calibrated test tube containing 800 μL of distilled water. After that, 60 μL of solution 1, 40 μL of solution 2 were introduced. Finally, the solution was thoroughly mixed and transferred for the UV-vis absorption spectra measurement after incubation at room temperature for 10 min.

Specifically, solution 1 was firstly prepared by addition of 1 g AA and 0.05 g EDTA into 20 mL of distilled water. Then 0.8 mL formic acid was added after the dissolution. Finally, distilled water was introduced to the above solution to fix the volume to 50 mL. Solution 2 was prepared by the following method. In detail, 1.3 g ammonium molybdate and 0.05 g potassium antimony tartrate were added to 23 mL of 50% H_2SO_4 solution. After the thorough dissolution, distilled water was introduced to the above solution to fix the volume to 50 mL.

Results and discussion

The mechanism of this assay for ALP and Na_3VO_4 detection

Previous reports have shown that nanoceria possess oxidase-like catalytic activity [23]. In this regard, we utilize TMB as the peroxidase substrate to investigate its catalytic behavior. TMB is colorless (a, inset of Fig. 1) and shows no obvious absorption peak in the wavelength ranging from 550 to 750 nm (a, Fig. 1). However, when nanoceria is introduced to the TMB solution, a slight blue color (c, inset of Fig. 1) with an absorption peak at 645 nm (c, Fig. 1) appears, suggesting the formation of oxTMB. Interestingly, when PPi is added into the nanoceria-TMB solution, both a deep blue color (d, inset of Fig. 1) and enhanced absorption intensity are observed (d, Fig. 1). As we known, PPi itself is not an oxidizing reagent and it cannot oxidize TMB. And thus, directly mixing PPi and TMB cannot result in either color change (b, inset of Fig. 1) or absorption peak (b, Fig. 1). Surprisingly, a slight blue color (e, inset of Fig. 1) and decreased absorption intensity (e, Fig. 1) are obtained after the addition of ALP. While when Na_3VO_4 is added to the above system, a dark blue color (f, inset of Fig. 1) and increased absorption intensity (f, Fig. 1) appears again.

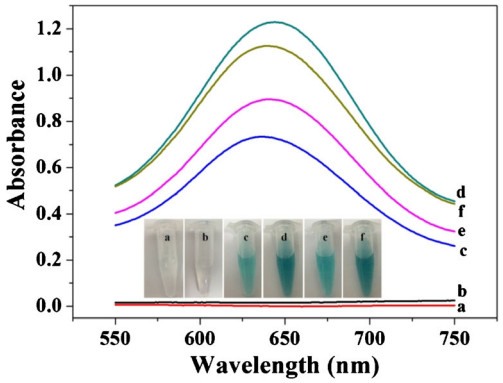

Fig. 1 UV-vis absorption spectra of TMB (**a**), TMB + PPi (**b**), TMB + nanoceria (**c**), TMB + nanoceria + PPi (**d**), TMB + nanoceria + PPi + ALP (**e**) and TMB + nanoceria + PPi + ALP + Na_3VO_4 (**f**). Inset shows the corresponding photos of the solutions under visible light. The final concentrations of the TMB, PPi, nanoceria, ALP and Na_3VO_4 are 0.5 mM, 70 μM, 0.25 mg mL^{-1}, 20 mU mL^{-1} and 0.1 mM, respectively

Moreover, it is well-studied that nanoceria shows phosphatase-like activity [27, 28], making it possible to catalyze the hydrolysis of PPi. We utilize standard molybdenum-blue method, which is based on the facts that the presence of phosphate ion (Pi) will induce an obvious absorption peak at 710 nm, to investigate the phosphatase-like activity of naoceria. When PPi (a, Fig. S2) or nanoceria (b, Fig. S2) is individually introduced into the solution, no absorption peak at 710 nm is observed. However, an obvious absorption peak at 710 nm is obtained when PPi and nanoceria are introduced simultaneously (c, Fig. S2). Moreover, enhanced absorption intensity is obtained when ALP and PPi were firstly incubated (d, Fig. S2). All these results show that Pi is liberated to the solution during the hydrolysis of PPi catalyzed by nanoceria. By the standard molybdenum-blue method, the amounts of Pi for the nanoceria-PPi and nanoceria-PPi-ALP are calculated to be 70.4 μM and 133.8 μM, respectively. Furthermore, we study the effects of 70.4 μM and 133.8 μM of Pi on the oxidase-like activity of nanoceria. As shown in Fig. S3, both of them show negligible impact on the oxidase-like activity of nanoceria. All the results above show that the inhibited oxidase-like activity of nanoceria after the introduction of ALP is unrelated to the increased concentrations of Pi.

On the basis of the above facts, a possible mechanism is proposed (Scheme 1). The hydrolysis process of PPi can be catalyzed in-situ by nanoceria with large energy release [29–31], which may enhance the oxidase-like activity and promote the oxidation reaction of TMB in return. On one hand, when ALP is firstly incubated with PPi, ALP can hydrolyze PPi toward to Pi, inhibiting the hydrolysis of PPi by nanoceria and the release of energy resulting in the inhibition of TMB oxidation. On the other hand, Na_3VO_4 can inhibit ALP activity, which promotes the oxidation of TMB again. However, the mechanism of PPi-promoted oxidase-like activity of nanoceria for ALP detection needs further study.

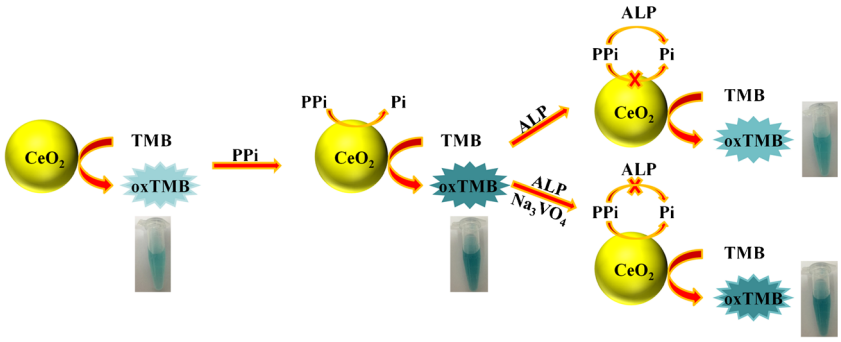

Scheme 1 Schematic illustration of the PPi-accelerating the oxidase-like activity of nanoceria for ALP activity and its inhibitor detection

Optimization of detection conditions

Several parameters are needed to optimize before the application of this assay for ALP detection, including the pH of acetate buffer, the concentrations of nanoceria and TMB, incubation temperature and time. Here, we utilize ΔA (A_0-A) as a criteria to obtain the optimum condition, where A_0 and A are the absorption intensity of nanoceria-TMB before and after the introduction of ALP, respectively.

The optimal detection conditions for ALP are as follows: (1) the pH of acetate buffer is 4.0 (Fig. S4), (2) the concentrations of nanoceria is 0.25 mg mL^{-1} (Fig. S5), (3) the concentrations of TMB is fixed at 0.5 mM (Fig. S6), (4) the incubation temperature is 37 °C (Fig. S7), (5) the incubation time is 3 min (Fig. S8).

Analytical performances of this assay for PPi and ALP detection

Under the optimized conditions, the analytical performances of this assay for PPi and ALP detection were systematically investigated. We firstly investigate the effect of PPi concentration on the oxidase-like activity of nanoceria. As shown in Fig. 2, obvious color changes from light blue to dark blue and drastic absorption intensity enhancement are found with the increasing concentration of PPi. It is found that the absorption intensity at 645 nm show a linear relationship with PPi concentration ranging from 5 to 70 μM. The regression equation is $\Delta A = 0.0095 + 0.0056c$ (c, PPi concentration, μM; $R^2 = 0.9896$), in which ΔA refers to the enhancement of absorption intensity at 645 nm after the introduction of PPi. Therefore, this assay can be utilized for PPi detection. It is believed higher PPi concentration can achieve better enhancement of the oxidase-like activity of nanoceria, however, it is not beneficial for the highly sensitive detection of ALP. Taken the good sensitivity into account, the final concentration of PPi in the following assays is set as 70 μM.

Then, this assay is further used for ALP detection. With the increasing ALP concentration, the absorption intensity decrease continually (Fig. 3a), while the ΔA increase gradually and keep almost unchanged when the concentration of ALP is higher than 10 mU mL^{-1} (Fig. 3b). It is clearly found that the color of the solution change from dark blue to light blue with the increasing ALP concentration and an obvious color changes is found when the concentration of ALP exceeds 4 mU mL^{-1} (inset of Fig. 3b), indicating the high sensitivity

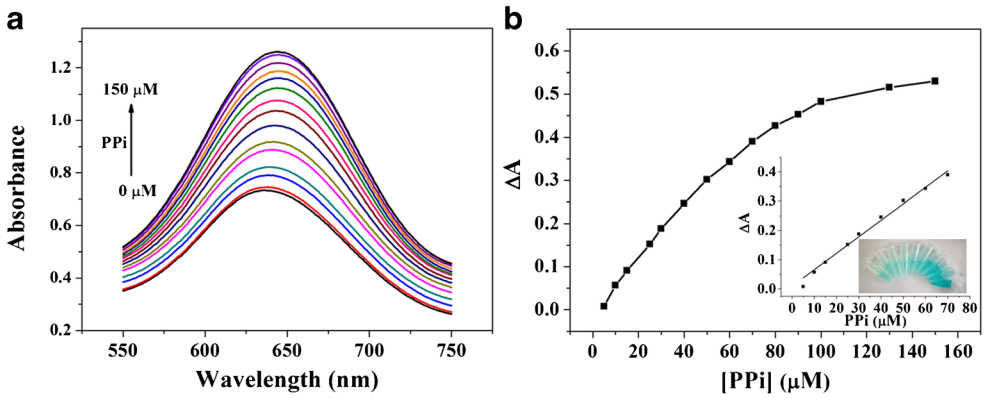

Fig. 2 **a** UV-vis absorption spectra of the nanoceria-TMB solution after the introduction of various concentrations of PPi (From down to top, the concentration of PPi are 0, 5, 10, 15, 25, 30, 40, 50, 60, 70, 80, 90, 100, 130, 150 μM). **b** PPi concentration dependent changes of the absorption intensity at 645 nm. Inset shows the relationship between the ΔA and PPi concentration and the color changes of nanoceria-TMB solution after the addition of PPi (from left to right, the concentration of PPi are 0, 5, 10, 15, 25, 30, 40, 50, 60, 70 μM)

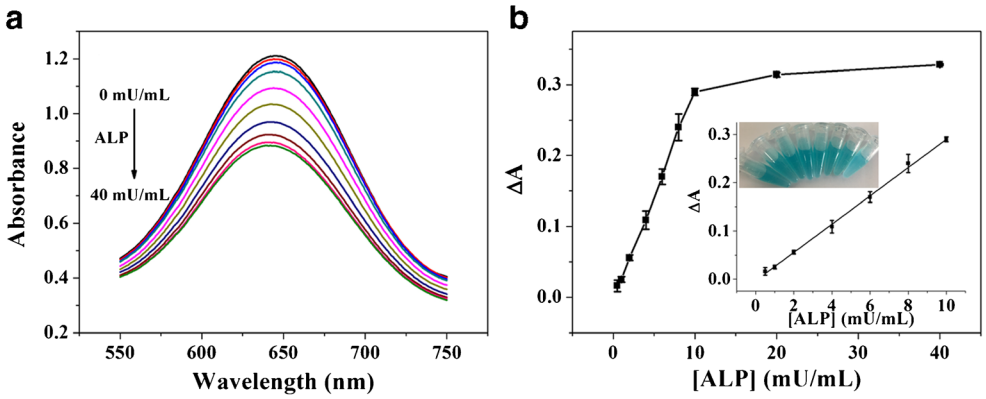

Fig. 3 **a** UV-vis absorption spectra of the nanoceria-TMB-PPi solution after the introduction of various concentrations of ALP (From top to down, the concentrations of ALP are 0, 0.5, 1, 2, 4, 6, 8, 10, 20 and 40 mU mL^{-1}). **b** ALP concentration dependent changes of the absorption intensity at 645 nm. Inset shows the relationship between the ΔA and ALP concentration and the color changes of nanoceria-TMB-PPi solution after the addition of ALP (from left to right, the concentration of ALP are 0, 0.5, 1, 2, 4, 6, 8, 10 mU mL^{-1}). Error bars illustrate the standard deviation of three independent measurements

of this assay. Moreover, a good linear relationship between ΔA and ALP concentration is obtained with a linear equation $\Delta A = -0.0031 + 0.0293c$ (c, ALP concentration, mU mL^{-1}; $R^2 = 0.9995$) when the ALP concentrations are in the range from 0.5 to 10 mU mL^{-1}. The detection limit for ALP activity detection is estimated to be 0.32 mU mL^{-1} at a signal-to-noise ratio of 3. In addition, we compare the analytical performances of this method with previously reported methods for ALP activity detection. As shown in Table S1, the linear range and detection limit of this method are comparable or even better than other methods. Furthermore, the short detection time (3 min) after incubation PPi and ALP for 1 h and obvious color changes of this assay may make it possible for ALP detection in real samples. To further evaluate its potential in practical application, detection of ALP in diluted human serum samples (1%) are carried out by using standard addition method. As shown in Table S2, recoveries are in the range from 86.3 to 109% with the relative standard deviation (RSD) less than 4.89%. The good recoveries and acceptable RSD indicate that this assay is promising for ALP detection in complicated biological samples.

In order to testify the specificity of this assay for ALP detection, we investigate the effects of BSA, lysozyme, pepsin, trypsin, pancreatin, thrombin, hemoglobin and bilirubin on the detection assay when they are added individually or coexistently with ALP. The results in Fig. 4 conceivably validate that none of them can induce absorption intensity changes in this detection system and show negligible impact on ALP detection. Consequently, this assay is highly selective for ALP detection.

ALP inhibitor screening

Since the inhibition of ALP activity is closely related to drug screening and disease therapy, we also explore the possibility of this assay for ALP inhibitor screening. Na_3VO_4, a typical and common inhibitor for ALP, is used as a model to study the inhibitory activity assay. The inhibition efficiency (IE) is calculated by the following equation: IE (%) = 100 × (A_i-A)/(A_0-A), where A_i represents the absorbance at 645 nm of nanoceria-TMB in the presence of PPi, PPi-ALP and PPi-ALP-Na_3VO_4. When Na_3VO_4 is introduced to the detection assay, the activity of ALP is inhibited and the hydrolysis of PPi is restricted, resulting in the absorption intensity recovery. As given in Fig. 5a, the absorbance at 645 nm increases continually with the increasing amounts of the added Na_3VO_4. The IC_{50} value (the concentration of Na_3VO_4 needed for 50% inhibition of ALP activity) is calculated to be 71 μM (Fig. 5b), which is close to those reported by other ALP activity assays [32, 33].

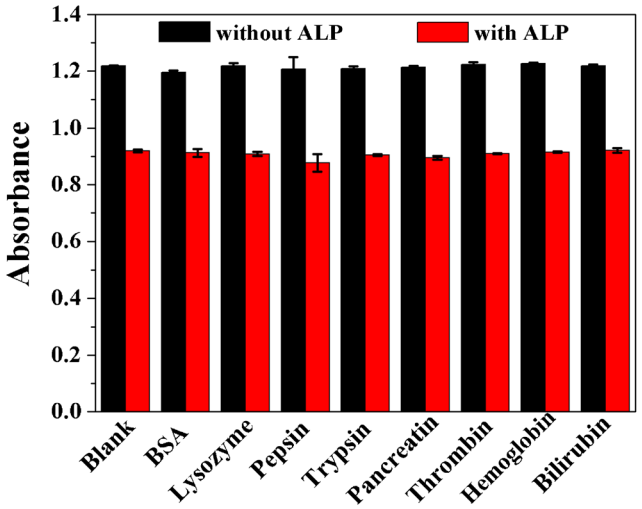

Fig. 4 The absorbance of nanoceria-TMB-PPi solution in the presence of these possible interfering substances only or coexistence with ALP. The final concentrations of these substances are 1 μg mL^{-1}. Error bars indicate the standard deviation of three independent measurements

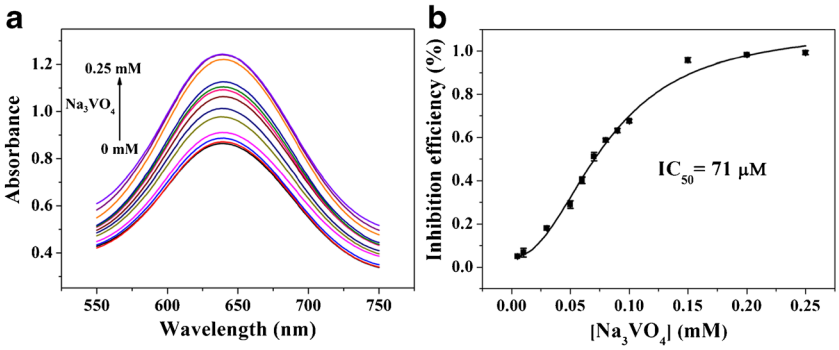

Fig. 5 **a** UV-vis absorption spectra of the solution prepared by addition of Na_3VO_4-treated ALP into the acetate buffer containing nanoceria-TMB-PPi. From down to top, the concentrations of Na_3VO_4 are 0, 0.005, 0.01, 0.03, 0.05, 0.06, 0.07, 0.08, 0.09, 0.1, 0.15, 0.20, 0.25 mM. **b** Plot of the IE versus Na_3VO_4 concentration. The final concentrations of TMB, PPi, nanoceria and ALP are 0.5 mM, 70 μM, 0.25 mg mL^{-1} and 20 mU mL^{-1}. Error bars demonstrate the standard deviation of three independent measurements

Conclusion

A highly sensitive assay for ALP and its inhibitor detection is successfully developed based on the finding that PPi can accelerate the oxidase-like activity of nanoceria. To the best of our knowledge, this assay shows several distinctive advantages as follows. (1) It is time-saving and cost-effective by mixing nanoceria, TMB and PPi together. (2) It shows high sensitivity and good selectivity for ALP detection. Therefore, this assay displays promising potential for detection of ALP in real samples. Moreover, it may not only provide a new approach to boost the mimetic enzyme activity of nanozymes but also make great contribution to explore the bioanalytical applications of nanoceria.

Acknowledgments This work was financially supported by the National Natural Science Foundation of China (21705056), the Young Taishan Scholars Program of Shandong Province (tsqn201812080), the program for Taishan Scholars of Shandong province (ts201712048), the Natural Science Foundation of Shandong Province (ZR2017MB022, ZR2018BB057 and ZR2018PB009) and the start-up funding from University of Jinan (511-1009408, 511-1009424).

Compliance with ethical standards The author(s) declare that they have no competing interests.

References

1. Li J, Si L, Bao J, Wang Z, Dai Z (2017) Fluorescence regulation of poly(thymine)-templated copper nanoparticles via an enzyme-triggered reaction toward sensitive and selective detection of alkaline phosphatase. Anal Chem 89:3681–3686
2. Coleman JE (1992) Structure and mechanism of alkaline phosphatase. Ann Rev Bioph Biom 21:441–483
3. Withold W, Schulte U, Reinauer H (1996) Method for determination of bone alkaline phosphatase activity: analytical performance and clinical usefulness in patients with metabolic and malignant bone diseases. Clin Chem 42:210–217
4. Fernandez NJ, Kidney BA (2007) Alkaline phosphatase: beyond the liver. Vet Clin Path 36:223–233
5. Ramaswamy G, Rao VR, Krishnamoorthy L, Ramesh G, Gomathy R, Renukadevi D (2000) Serum levels of bone alkaline phosphatase in breast and prostate cancers with bone metastasis. Indian J Clin Biochem 15:110–113
6. Tibi L, Collier A, Patrick AW, Clarke BF, Smith AF (1988) Plasma alkaline phosphatase isoenzymes in diabetes mellitus. Clin Chim Acta 177:147–155
7. Zhang Z, Chen Z, Wang S, Cheng F, Chen L (2015) Iodine-mediated etching of gold nanorods for plasmonic elisa based on colorimetric detection of alkaline phosphatase. ACS Appl Mater Interfaces 7:27639–27645
8. Park CS, Ha TH, Kim M, Raja N, H-s Y, Sung MJ, Kwon OS, Yoon H, Lee C-S (2018) Fast and sensitive near-infrared fluorescent probes for ALP detection and 3d printed calcium phosphate scaffold imaging in vivo. Biosens Bioelectron 105:151–158
9. Goggins S, Naz C, Marsh BJ, Frost CG (2015) Ratiometric electrochemical detection of alkaline phosphatase. Chem Commun 51:561–564
10. Zeng Y, Ren J-Q, Wang S-K, Mai J-M, Qu B, Zhang Y, Shen A-G, Hu J-M (2017) Rapid and reliable detection of alkaline phosphatase by a hot spots amplification strategy based on well-controlled assembly on single nanoparticle. ACS Appl Mater Interfaces 9:29547–29553
11. Zhang Q, Zhang C, Yang M, Yu D, Yu C (2017) Pyrophosphate as substrate for alkaline phosphatase activity: a convenient flow-injection chemiluminescence assay. Luminescence 32:1150–1156
12. Bowers GN, McComb RB (1966) A continuous spectrophotometric method for measuring the activity of serum alkaline phosphatase. Clin Chem 12:70–89
13. Gao Z, Deng K, Wang X-D, Miro M, Tang D (2014) High-resolution colorimetric assay for rapid visual readout of phosphatase activity based on gold/silver core/shell nanorod. ACS Appl Mater Interfaces 6:18243–18250
14. Guo Y, Wu J, Li J, Ju H (2016) A plasmonic colorimetric strategy for biosensing through enzyme guided growth of silver nanoparticles on gold nanostars. Biosens Bioelectron 78:267–273
15. Shi D, Sun Y, Lin L, Shi C, Wang G, Zhang X (2016) Naked-eye sensitive detection of alkaline phosphatase (ALP) and pyrophosphate (PPi) based on a horseradish peroxidase catalytic colorimetric system with cu(II). Analyst 141:5549–5554

16. Wei H, Wang E (2013) Nanomaterials with enzyme-like characteristics (nanozymes): next-generation artificial enzymes. Chem Soc Rev 42:6060–6093
17. Wu J, Wang X, Wang Q, Lou Z, Li S, Zhu Y, Qin L, Wei H (2019) Nanomaterials with enzyme-like characteristics (nanozymes): next-generation artificial enzymes (II). Chem Soc Rev 48:1004–1076
18. Wang C, Gao J, Cao Y, Tan H (2018) Colorimetric logic gate for alkaline phosphatase based on copper (II)-based metal-organic frameworks with peroxidase-like activity. Anal Chim Acta 1004: 74–81
19. Yang J, Zheng L, Wang Y, Li W, Zhang J, Gu J, Fu Y (2016) Guanine-rich DNA-based peroxidase mimetics for colorimetric assays of alkaline phosphatase. Biosens Bioelectron 77:549–556
20. Liu Y, Wang J, Song X, Xu K, Chen H, Zhao C, Li J (2018) Colorimetric immunoassay for listeria monocytogenes by using core gold nanoparticles, silver nanoclusters as oxidase mimetics, and aptamer-conjugated magnetic nanoparticles. Microchim Acta 185:360
21. Ge J, Xing K, Geng X, Hu Y, Shen X, Zhang L, Li Z-H (2018) Human serum albumin templated MnO_2 nanosheets are oxidase mimics for colorimetric determination of hydrogen peroxide and for enzymatic determination of glucose. Microchim Acta 185:559
22. Wang C, Tang G, Tan H (2018). Colorimetric determination of mercury(II) via the inhibition by ssDNA of the oxidase-like activity of a mixed valence state cerium-based metal-organic framework. Microchim Acta185:475
23. Asati A, Santra S, Kaittanis C, Nath S, Perez JM (2009) Oxidase-like activity of polymer-coated cerium oxide nanoparticles. Angew Chem Int Ed 48:2308–2312
24. Liu B, Huang Z, Liu J (2016) Boosting the oxidase mimicking activity of nanoceria by fluoride capping: rivaling protein enzymes and ultrasensitive F^- detection. Nanoscale 8:13562–13567
25. Cheng H, Lin S, Muhammad F, Lin Y-W, Wei H (2016) Rationally modulate the oxidase-like activity of nanoceria for self-regulated bioassays. ACS Sens 1:1336–1343
26. Huang L, Zhang W, Chen K, Zhu W, Liu X, Wang R, Zhang X, Hu N, Suo Y, Wang J (2017) Facet-selective response of trigger molecule to CeO_2 {110} for up-regulating oxidase-like activity. Chem Eng J 330:746–752
27. Xu C, Liu Z, Wu L, Ren J, Qu X (2014) Nucleoside triphosphates as promoters to enhance nanoceria enzyme-like activity and for single-nucleotide polymorphism typing. Adv Funct Mater 24: 1624–1630
28. Yao T, Tian Z, Zhang Y, Qu Y (2019) Phosphatase-like activity of porous nanorods of CeO_2 for the highly stabilized dephosphorylation under interferences. ACS Appl Mater Interfaces 11:195–201
29. Reeves RE, South DJ, Blytt HJ, Warren LG (1974) Pyrophosphate: D-fructose 6-phosphate 1-phosphotransferase. A new enzyme with the glycolytic function of 6-phosphofructokinase. J Biol Chem 249: 7737–7741
30. Takeshige K, Tazawa M (1989) Determination of the inorganic pyrophosphate level and its subcellular localization in Chara corallina. J Biol Chem 264:3262–3266
31. Wang X, Lopez A, Liu J (2018) Adsorption of phosphate and polyphosphate on nanoceria probed by DNA oligonucleotides. Langmuir 34:7899–7905
32. Chen Y, Li W, Wang Y, Yang X, Chen J, Jiang Y, Yu C, Lin Q (2014) Cysteine-directed fluorescent gold nanoclusters for the sensing of pyrophosphate and alkaline phosphatase. J Mater Chem C 2: 4080–4085
33. Xu A-Z, Zhang L, Zeng H-H, Liang R-P, Qiu J-D (2018) Fluorometric determination of the activity of alkaline phosphatase based on the competitive binding of gold nanoparticles and pyrophosphate to $CePO_4$:Tb nanorods. Microchim Acta 185:288